



HAL
open science

Brain accumulation of inhaled uranium in the rat depends on aerosol concentration, exposure repetitions, particle size and solubility

Benjamin Tournier, Chrystelle Ibanez, Elie Tournalonias, Fabrice Petitot, Francois Paquet, Isabelle Dublineau, Philippe Lestaevel

► To cite this version:

Benjamin Tournier, Chrystelle Ibanez, Elie Tournalonias, Fabrice Petitot, Francois Paquet, et al.. Brain accumulation of inhaled uranium in the rat depends on aerosol concentration, exposure repetitions, particle size and solubility. *Toxicology Letters*, 2021, pp.10-17. 10.1016/j.toxlet.2021.08.002 . hal-03409664

HAL Id: hal-03409664

<https://hal.science/hal-03409664v1>

Submitted on 22 Aug 2023

HAL is a multi-disciplinary open access archive for the deposit and dissemination of scientific research documents, whether they are published or not. The documents may come from teaching and research institutions in France or abroad, or from public or private research centers.

L'archive ouverte pluridisciplinaire **HAL**, est destinée au dépôt et à la diffusion de documents scientifiques de niveau recherche, publiés ou non, émanant des établissements d'enseignement et de recherche français ou étrangers, des laboratoires publics ou privés.



Distributed under a Creative Commons Attribution - NonCommercial 4.0 International License

1 **Brain accumulation of inhaled uranium in the rat depends on aerosol concentration, exposure repetitions,**
2 **particle size and solubility.**

3

4 Benjamin B. Tournier^{1,2}, Chrystelle Ibanez¹, Elie Tourlonias^{1,3}, Fabrice Petitot^{1,4}, François Paquet^{1,5}, Isabelle
5 Dublineau^{1,6}, Philippe Lestaevel^{1,7*}

6

7 ¹ Institut de Radioprotection et de Sûreté Nucléaire (IRSN), PSE-SANTE, SESANE, Laboratoire de
8 Radiotoxicologie et Radiobiologie Expérimentale, 92262 Fontenay-aux-Roses, France.

9 ² Division of Adult Psychiatry, Department of Psychiatry, University Hospitals of Geneva, Switzerland.

10 ³ Nucléagis SAS, 63480 Vertolaye, France.

11 ⁴ CEA, DEN, DUSP, Service de Protection contre les Rayonnements, 30207 Bagnols sur Cèze Cedex, France.

12 ⁵ Institut de Radioprotection et de Sûreté Nucléaire (IRSN), PSE-ENV, SRTE, 13115 Saint Paul-lez-Durance,
13 Cedex, France.

14 ⁶ Institut de Radioprotection et de Sûreté Nucléaire (IRSN), PSE-ENV, SEDRE, Unité d'expertise des sites et
15 des déchets radioactifs, 92262 Fontenay-aux-Roses, France.

16 ⁷ Institut de Radioprotection et de Sûreté Nucléaire (IRSN), PSE-SANTE, SER, Bureau d'Analyse et de Suivi
17 des Expositions Professionnelles, 92262 Fontenay-aux-Roses, France.

18

19 *Corresponding author:

20 Philippe Lestaevel

21 Institut de Radioprotection et de Sûreté Nucléaire (IRSN)

22 PSE-SANTE, SESANE, Laboratoire de Radiotoxicologie et Radiobiologie Expérimentale, Fontenay-aux-Roses,

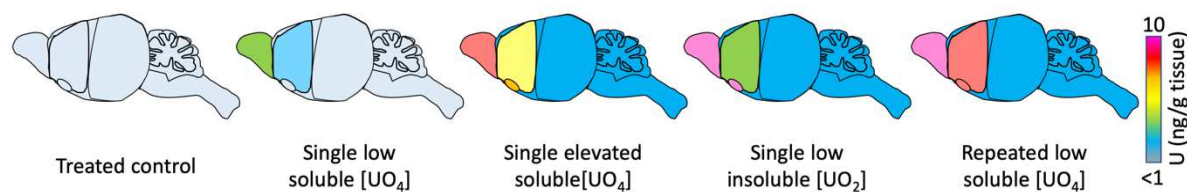
23 92262, France

24 Tel : +33 1 58 35 80 42

25 philippe.lestaevel@irsn.fr

26 **Graphical abstract.**

27



31 **Abstract.**

32 A rostro-caudal gradient of uranium (U) in the brain has been suggested after its inhalation. To study the factors
33 influencing this mapping, we first used 30-min acute inhalation at 56 mg/m³ of the relatively soluble form UO₄
34 in the rat. These exposure parameters were then used as a reference in comparison with the other experimental
35 conditions. Other groups received acute inhalation at different concentrations, repeated low dose inhalation of
36 UO₄ (10 exposures) or acute low dose inhalation of the insoluble form UO₂. At 24 hours after the last exposure,
37 all rats showed a brain U accumulation with a rostro-caudal gradient as compared to controls. However, the total
38 concentration to the brain was greater after repeated exposure than acute exposure, demonstrating an
39 accumulative effect. In comparison with the low dose soluble U exposure, a higher accumulation in the front of
40 the brain was observed after exposure to higher dose, to insoluble particles and following repetition of
41 exposures, thus demonstrating a dose effect and influences of solubility and repetition of exposures. In the last
42 part, exposure to ultrafine U particles made it possible to show 24 hours after exposure the presence of U in the
43 brain according to a rostro-caudal gradient. Finally, the time-course after exposure to micronic or nanometric U
44 particles has revealed greater residence times for nanoparticles.

45

46

47 **Keywords.**

48 Uranium, inhalation, nanoparticles, solubility, rat

49

50 **Abbreviations.**

51 BRes, brain residue; FCx, frontal cortex; Ins., insoluble; NT, nasal turbinates; OB, olfactory bulbs; OT, olfactory
52 tubercles; Rep., repeated exposures; UFP, ultrafine particles; WB, whole brain.

53 **1. Introduction.**

54 Uranium (U) is a natural radioactive transuranic element with a wide range of industrial uses, but its main
55 application concerns energy production and military use (Craft et al., 2004). The natural fissile isotope uranium-
56 ²³⁵U is used primarily in most nuclear power plants. The preparation of uranium to be used as fuel in nuclear
57 power plants includes different successive steps (mining, milling, conversion, enrichment, fabrication of nuclear
58 fuel and reprocessing in some cases). Importantly, depending on the steps in the uranium fuel cycle, the chemical
59 nature of U compounds, notably solubility, varies. Ammonium diuranate (NH₄)₂U₂O₇, a component of
60 yellowcake, is converted to uranium hexafluoride (UF₆) prior to ²³⁵U enrichment. The enriched UF₆ is then
61 converted into UO₂, the final product in the manufacture of nuclear fuel pellets used in most reactors
62 (UNSCEAR, 2016). In nuclear fuel cycle facilities, workers involved in the concentration or enrichment process
63 and in fuel fabrication could face repeated inhalations of airborne U compounds (Fulco et al., 2000). Indeed, dust
64 inhalation is one of the major risk of contamination for nuclear workers (Blanchin et al., 2004; Durakovic et al.,
65 2003; Fulco et al., 2000; Salbu et al., 2005). Furthermore, in addition to micrometric U dusts, metal ultrafine or
66 nanometric (<100 nm) U particles can be also generated as byproducts in several industrial steps of the nuclear
67 fuel cycle or during the decommissioning of nuclear facilities (Dewalle et al., 2010; Onodera et al., 1991;
68 Trelenberg et al., 2006).

69 After inhalation, the first organs impacted by the uranium deposition are the lungs as described in the Human
70 Respiratory Tract Model (HRTM biokinetic model) (ICRP, 1994). Accordingly to their pulmonary transfer rate,
71 uranium compounds can be classified according to their solubility as fast (F), moderate (M) and slow (S) (ICRP,
72 2017). As an example, the solubility of UO₄ is 50% type F and 50% type M. The ICRP model aims at predicting
73 translocation and deposition of uranium according to particle size parameters and then subsequent retention
74 following its deposition depending on the different anatomical pulmonary regions (bronchial and alveolar
75 compartments). U distribution is then predicted by the systemic biokinetic model to the whole organism *via* the
76 blood pathway. After its absorption to blood, uranium is present mainly as uranyl ions complexed to proteins
77 (e.g. transferrin, albumin) or bicarbonate anions (Ansoborlo et al., 2006). The main sites of deposition of
78 uranium from the circulation are the skeleton and the kidneys. In addition, experimental data predict that part of
79 the metal enters the brain (Ballou et al., 1986; Diamond et al., 1989; La Touche et al., 1987; Lemerrier et al.,
80 2003). Most recently, several publications suggested that uranium deposition in brain is higher after inhalation
81 than after ingestion or injection, suggesting that the cerebral accumulation of U depends on the mode of
82 contamination (for review, see (Dinocourt et al., 2015)). For instance, 24 hours after the end of repeated

83 inhalations in rat, the total brain U amounts were about 0.47% of the total U retained in the body but they were
84 only about 0.007 and 0.24% after respectively an acute injection or chronic ingestion (Houpert et al., 2007).

85 In addition, compared to other modes of exposure, inhalation of U resulted in the presence of an important
86 rostro-caudal gradient with the olfactory bulbs containing the highest concentration (Barber et al., 2005; Houpert
87 et al., 2007; Houpert et al., 2005; Monleau et al., 2005; Paquet et al., 2006; Tournier et al., 2009). A direct
88 transfer from the nasal cavity to the brain have been proposed to explain such a heterogeneous brain distribution
89 (Ibanez et al., 2019; Ibanez et al., 2014; Tournier et al., 2009). This additional route of entry to the brain without
90 transit through the lungs and bloodstream in rats appears to modify the U brain mapping which, if it exists in
91 humans, could also represent a new mode of contamination for U particles that is not taken in account in the
92 HRTM ICRP model. Therefore, the knowledge of the brain distribution of inhaled U, which may depend on its
93 solubility, granulometry and concentration, is of importance in the case of U intoxication via inhalation.

94 The objective of this study was to highlight the link between physical-chemical characteristics of uranium
95 and the uranium distribution into the brain after inhalation. Specifically, the aims of our study were to compare
96 different U aerosol inhalation protocols on resulting concentrations in some brain parts, using soluble (F/M) and
97 insoluble (M/S) forms of uranium, acute or repeated exposure mode, micronic or nanometric U particles. To this
98 end, a first group was exposed acutely to a “low” concentration of soluble U aerosol (UO_4) The term “low” is
99 then used as a reference term and is indicated as “low” in terms of aerosol volumic concentration and in
100 comparison with the other experimental conditions exposed to a higher concentration. The frontal cortex,
101 olfactory bulbs and tubercles and the rest of the brain were used as a reference brain map. The distribution of the
102 inhaled U was then compared with other groups having inhaled acutely the same aerosol (UO_4) but at higher
103 dose, or having inhaled acutely an aerosol formed a less soluble U physico-chemical form (UO_2) at low dose.
104 Another group was then exposed repeatedly at the same low dose of the same soluble aerosol (UO_4 , 10
105 exposures). In a second part, the entry to the brain of U nanoparticles (UO_2) was sought. Finally, the kinetics of
106 retention of U in the brain was compared between two U aerosols formed of whether nanoparticles or
107 microparticles.

108 **2. Material and methods.**

109

110 *2.1. Animals*

111 Adult male Sprague–Dawley rats (Charles River Laboratories, France) were housed in pairs under standard
 112 conditions (light on: 8.00 am/8.00 pm; temperature: 22 ± 1 ° C) with food (105, CERJ, France) and water
 113 provided *ad libitum* and were randomly assigned to one of the experimental groups (n=8/group). Group details
 114 are given in the table 1. To avoid stress, rats were progressively acclimatized to the nose-only exposure tubes
 115 over a three-week period. Treated control rats have also performed the habituation to the nose-only exposure
 116 tubes and were only exposed to ambient air. All animal procedures were approved by the Animal Care
 117 Committee of the IRSN and complied with French regulations for animal experimentation (Ministry of
 118 Agriculture Act N°87-848, October 19th 1987, modified 29th of May 2001. They were approved by the IRSN
 119 Ethics Committee and authorized by the French Ministry of Research.

120

Group name	Low	High	Ins.	Rep.	UFP
	Micrometric aerosol				Nanometric aerosol
Chemical form	UO ₄	UO ₄	UO ₂	UO ₄	UO ₂
ICRP reference absorption type	Intermediate type F/M	Intermediate type F/M	Intermediate type M/S	Intermediate type F/M	Intermediate type M/S
Aerosol concentration (mg/m ³)	56 ±28	<u>412 ±82</u>	52 ±14	61 ±17	<u>1 ±0</u>
Duration of the exposure (min)	30	30	30	30	<u>60</u>
Number of exposures	1	1	1	10 (3x/wk)	1
Mass median aerodynamic diameter (µm) (range)	1.99 ±0.13 (1.72-2.2)	1.79 ±0.07 (1.71-2.1)	1.81 ±0.02 (1.74-1.83)	1.64 ±0.17 (1.47-2-2)	0.15 ±0.09 (0.08-0.3)
Radiological nature	Reprocessed	Reprocessed	Depleted	Reprocessed	Depleted
Isotopic ratio	²³⁸ U = 99.55% ²³⁶ U = 0.051% ²³⁵ U = 0.39% ²³⁴ U = 0.0047%	²³⁸ U = 99.55% ²³⁶ U = 0.051% ²³⁵ U = 0.39% ²³⁴ U = 0.0047%	²³⁸ U = 99.75% ²³⁵ U = 0.24% ²³⁴ U = 0.001%	²³⁸ U = 99.55% ²³⁶ U = 0.051% ²³⁵ U = 0.39% ²³⁴ U = 0.0047%	²³⁸ U = 99.799% ²³⁵ U = 0.200% ²³⁴ U = 0.001%

121 **Table 1. Characteristics of uranium aerosols.** Characteristics of uranium used in the present study for aerosol
 122 generation as well as some parameters of animal exposure design are indicated in this table. Data are indicated
 123 as mean ±SD. Abbreviations: Ins., insoluble; Rep., repeated exposures; UFP, ultrafine particles. ICRP reference
 124 absorption types: F: fast; M: moderate; S: slow (from ICRP 137, 2017).

125

126

127 2.2. *Aerosol generation*

128 The aerosol generation and the measure of their characteristics were previously described (Petitot et al., 2013;
129 Tournier et al., 2009). Industrial U dioxide (UO₂) and U peroxide (UO₄) powders found at workplaces in U fuel
130 cycle facilities were supplied by ORANO-AREVA NC (Pierrelatte, France). Briefly, micronic UO₄ and UO₂
131 aerosols were generated from uranium powder with the RBG1000 rotating brush generator (PALAS®, France)
132 used for aerosol generation from dry powder. The isotopic composition by mass of the UO₄ powder was ²³⁸U=
133 99.55%; ²³⁶U= 0.051%; ²³⁵U= 0.39%; ²³⁴U= 0.0047%. Microparticle aerosol concentrations, particle size
134 distribution and their mass median aerodynamic diameter were monitored using an aerodynamic particle sizer
135 (APS 3321, Trust Science Innovation, TSI®, France) combined with a diluter, as previously described (Monleau
136 et al., 2006; Tournier et al., 2009).

137 Nanoparticles aerosol was generated using a uranium metal bar and the spark-discharge aerosol generator
138 (PALAS GFG 1000). Nanoparticle aerosol concentrations and their mass median aerodynamic diameter were
139 determined using a filter sampling unit and a differential mobility analyzer (DMA, TSI®) combined with a
140 condensation particle counter (CNC, TSI®). To avoid saturation of the measuring devices, a dilution system of
141 the aerosol (VKL100, 2 bar) was installed upstream of the Scanning Mobility Particle Sizer (i.e. DMA + CNC)
142 (Petitot et al., 2013). The characteristics of the aerosols are given in Table 1. The uranium concentrations used
143 here in microparticle aerosols are lower than those previously used showing none effects on general health and
144 blood-plasma biochemical parameters (Monleau et al., 2006; Monleau et al., 2005; Tournier et al., 2009). More
145 details on the characterization of nanoparticles such as the ultrastructure of the uranium particles contained in the
146 air stream from the inhalation chamber and the elemental composition of these particles were published
147 previously (Petitot et al., 2013).

148

149 2.3. *Inhalation exposures*

150 Aerosol exposures were performed using the nose-only inhalation system contained within a glove box, a
151 procedure previously described (Monleau et al., 2005). The nose-only inhalation system is composed of three
152 parts: the aerosol generation part with the generators (RBG or PALAS), the metrology part containing the
153 devices used to perform real time monitoring (APS or SMPS), and the inhalation chamber itself on which the
154 nose-only tubes can be connected. Before uranium inhalation exposure, all animals are progressively
155 acclimatized to the tubes as mentioned previously. The noses of the rats contained within the tubes are then in
156 direct contact with the aerosols generated inside this inhalation chamber. At the end of each exposure, the nose

157 of each animal was washed to remove residues of U particles, in order to eliminate any risk of ingestion. The
158 characteristics of aerosols and exposures are indicated in the Table 1. All exposed groups were associated with a
159 respective treated control group (i.e. exposed to ambient air).

160

161 2.4. *Sample collection*

162 Deeply isoflurane anaesthetized (inhalation of isoflurane 5% / air 95%) rats were euthanized and their brain
163 quickly removed. The olfactory bulbs, olfactory tubercles, frontal cortex and the rest of the brain (indicated in
164 the rest of the document as “brain residue”) were dissected out on ice, weighed and stored at -80°C until
165 required. Peripheral organs (nasal turbinates and kidneys) were also dissected on ice, weighed and stored at
166 -80°C .

167

168 2.5. *Uranium measurements using an inductively coupled plasma mass spectrometer*

169 Uranium concentration analyses were performed as previously reported (Ibanez et al., 2019). Selected brain
170 areas and peripheral organs were digested using 8 mL nitric acid HNO_3 (Ultrapur, JT Becker) and 2 mL of 30%
171 hydrogen peroxide (Normapur, VWR) in a microwave oven (Milestone StartD microwave digestion system 1000
172 W, Ethos TC; Milestone, Italy) as follows: 20 min to reach 200°C and then held at 200°C for 10min in the
173 microwave oven at 1000 W using the digestion rotor system. Samples were then evaporated and dissolved in 5
174 ml of 10% HNO_3 . Samples were diluted and elemental uranium concentration was measured using an
175 inductively coupled plasma mass spectrometer (ICP-MS, PQ EXCELL, ThermoElectron with S-Option) using
176 bismuth as the internal standard (Claritas PPT Grade). The detection limit of uranium measured was: 1 ng/L for
177 ^{238}U and ^{235}U .

178

179 2.6. *Statistics*

180 The whole brain U concentration was compared between groups using a one-way ANOVA with the LSD *post*
181 *hoc* test. Two-way ANOVA with the LSD *post hoc* test were used to estimate differences in uranium
182 concentrations in rat cerebral areas (treatment and cerebral areas as factors) and to analyze the kinetics of U in
183 the brain (treatment and time as factors).

184 **3. Results**

185

186 **3.1. Unexposed animals**

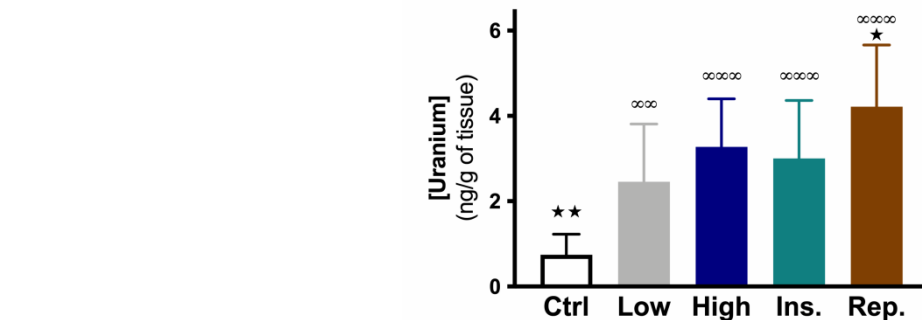
187

188 Control groups were used at each aerosol exposure experiment type (low, high, insoluble and repeated). No
189 difference was measured between them in terms of uranium concentration (see Supplemental table 1). Thus, data
190 from these groups were consequently pooled as a single control group. However, the statistical analysis was
191 doubly performed, considering the respective control group of each exposure experiment type and considering
192 the overall control group. The data presented below relate to comparisons with the pooled control group unless
193 otherwise indicated.

194

195 **3.2. Uranium concentration in the whole brain**

196 The experimental design showing aerosols characteristics and exposure modes are indicated in the Table 1:
197 animals received acute exposure to a low concentration of UO_4 (Low group), acute exposure to an elevated
198 concentration of UO_4 (High group), acute exposure to a low concentration of the insoluble UO_2 (Ins. group) or
199 repeated exposure to a low concentration of UO_4 (Rep. group). As compared to control animals, all groups
200 exposed to microparticles of uranium showed increased brain U concentrations (Low: +230%, $p < 0.01$; High:
201 +340%, $p < 0.001$; Ins.: +300%, $p < 0.001$, Rep.: +465%, $p < 0.001$) (Figure 1). Concerning differences between
202 uranium treated groups, the group exposed repeatedly to UO_4 showed higher U levels in comparison with the
203 acute exposure to a low concentration of UO_4 (+72%, $p < 0.05$). Raw data are given in the Supplemental Table 2.



204

205 **Figure 1. Uranium concentrations in the whole brain at 24h after inhalation.** Uranium concentrations were
206 measured in the whole brain and expressed as fold change in comparison with animals exposed to the low
207 concentration of UO_4 (Low group). Animals were exposed to a low concentration of soluble uranium (Low), to a
208 high concentration of soluble uranium (High), to a low concentration of insoluble uranium (Ins.) or to repeated
209 exposures of soluble uranium at a low concentration (Rep.). Data are given as mean \pm SD of 8 animals (control:

210 28 animals). Significant differences from the Low group are indicated at * $p < 0.05$ and ** $p < 0.01$ and from the
211 control group at $^{\infty}p < 0.01$ and $^{\infty\infty}p < 0.001$, using one-way ANOVA (treatment as factor) with the LSD *post hoc*
212 test.

213

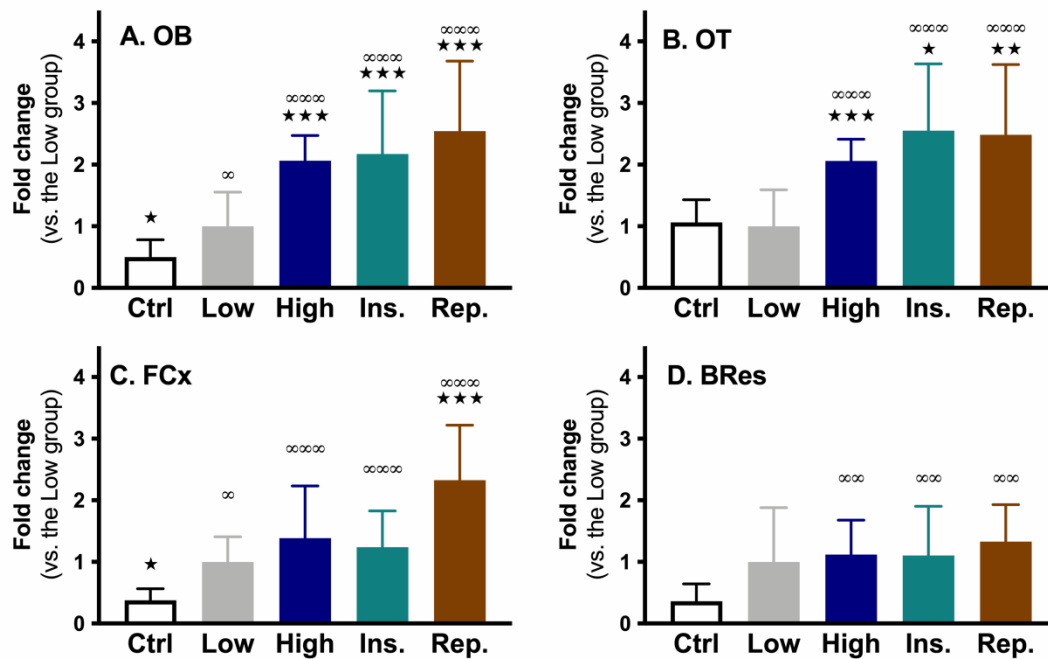
214 **3.3. Uranium concentration depends on the exposure mode.**

215 In comparison with controls, increases in U concentrations in olfactory bulbs (OB), olfactory tubercles (OT),
216 frontal cortex (FCx) and brain residue was observed in the High, the Insoluble and the Repeated groups (from
217 $p < 0.05$ to $p < 0.001$, Fig. 2). In main contrast, increases in U concentrations in the Low group were restricted to
218 OB ($p < 0.05$) and FCx ($p < 0.05$), suggesting a rostro-caudal gradient of U levels, as OB and FCx are more rostral
219 than OT and the rest of the brain (brain residue, BRes). A significant difference in U levels between OB and
220 BRes was observed in the High ($p < 0.001$), the Insoluble ($p < 0.05$) and the Repeated groups ($p < 0.05$).

221 In addition, a minimum of 2-fold increase in U levels in the OB and the OT was observed in the High, the
222 Insoluble and the Repeated groups, as compared to the Low group (from $p < 0.05$ to $p < 0.001$) (Fig. 2A-B). In the
223 frontal cortex (FCx), an increase in U levels was observed in animals repeatedly exposed to UO_4 as compared to
224 the Low group (2.3-fold change, $p < 0.001$, Fig. 2C). In the brain residue, there was no difference between groups
225 of various exposure modes (Fig. 2D). Raw data are given in the Supplemental Table 2.

226 In all exposed groups, the levels of U were increased in the nasal turbinates and the kidneys as compared to
227 controls (see Supplemental Table 2). In addition, a significant increase in U concentration was observed in the
228 nasal turbinates in the High group (+660%) and in the kidneys in the High (+2050%) and the Repeated (+680%)
229 groups, as compared to the Low group (Supplemental Table 2).

230



231

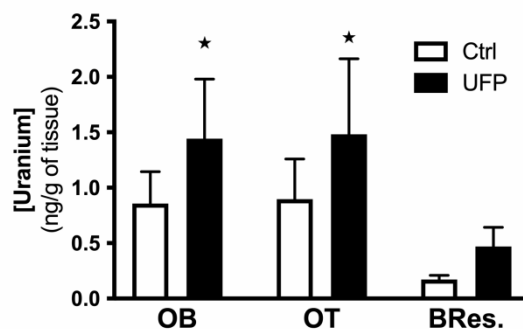
232 **Figure 2. Uranium concentrations in rat cerebral areas at 24h after inhalation.** Uranium concentrations
 233 were measured in olfactory bulbs (OB, **A**), olfactory tubercles (OT, **B**), frontal lobe of the cortex (FCx, **C**) and in
 234 brain residue (BRes, **D**). Animals were exposed to a low concentration of soluble uranium (Low), to a high
 235 concentration of soluble uranium (High), to repeated exposures of soluble uranium at a low concentration (Rep.)
 236 or to a low concentration of insoluble uranium (Ins.). Data are given as mean \pm SD of 8 animals. The groups of
 237 control animals (exposed to ambient air) corresponding to each experimental group are represented together due
 238 to the absence of difference between them (Ctrl, mean \pm SEM of 28 animals). Significant differences from the
 239 control group are indicated at $^{\infty}p<0.05$, $^{\infty\infty}p<0.01$ and $^{\infty\infty\infty}p<0.001$ and significant differences from the group
 240 exposed to a low concentration of soluble uranium (Low) are indicated at $*p<0.05$, $**p<0.01$ and $***p<0.001$
 241 using two-way ANOVA (treatment x brain region) with the LSD *post hoc* test.

242

243 3.4. Cerebral distribution of the inhaled ultrafine particles of uranium at 24h after exposure.

244 A group was exposed to nanometric uranium UO₂ aerosol. The characteristics of this aerosol and of its exposure
 245 mode are given in the Table 1. The Figure 3 shows the significant higher accumulation of U in OB (+68%,
 246 $p<0.05$) and OT (+65%, $p<0.05$) which is absent in the brain residue 24 hours after inhalation of UFP as
 247 compared with the 1-hour ambient air group.

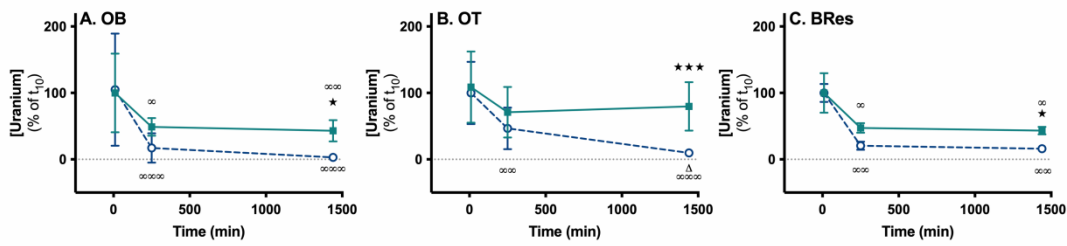
248



249
 250 **Figure 3. Uranium concentrations at 24h after inhalation of Uranium nanoparticles.** Animals were exposed
 251 to ambient air (open bars) or to ultra-fine particles of uranium (UFP, black bars). Data are given as mean \pm SD of
 252 8 animals. Significant differences from control are indicated at * $p < 0.05$. *Abbreviations:* BRes, brain residue;
 253 OB, olfactory bulbs; OT, olfactory tubercles.

255 3.5. Kinetics of U concentrations in the brain, following acute exposure to micronic or nanometric 256 particles of uranium.

257 Data showing uranium concentrations in OB, OT, and BRes at 10 min, 250 min, and 24 h after the end of the
 258 exposure to microparticles (UO_4) or to nanoparticles (U metal) are shown in Figure 4. In OB, as compared to the
 259 respective timepoint t_{10min} , U levels are significantly lower at t_{250min} and t_{24h} for both micro- and nanoparticles
 260 group ($p < 0.05$, $p < 0.01$ and $p < 0.001$). However, the U concentration decrease in OB for micronic particles is
 261 greater compared to nanoparticles, resulting in a significant difference between the two types of particles at t_{24h}
 262 ($p < 0.05$). At 24h post-exposure, U nanoparticle concentration is higher compared to microparticle one. In OT,
 263 levels of U microparticles decreased between t_{10min} and t_{250min} ($p < 0.01$) and between t_{250min} and t_{24h} ($p < 0.05$). In
 264 marked contrast, the concentration of U nanoparticles in OT remains stable throughout the measurement period,
 265 and result in a significant difference ($p < 0.001$) between the two types of particles at t_{24h} with significant higher U
 266 concentration for the nanoparticle group. In the BRes, kinetics were identical to those observed in the OB: a
 267 significant decrease between t_{10min} and t_{250min} and t_{10min} and t_{24h} ($p < 0.05$, $p < 0.01$) for both types of particles. A
 268 significant difference between the two types of particles is also observed at t_{24h} with higher U nanoparticles
 269 concentration as compared to microparticles ($p < 0.05$).



271

272 **Figure 4. Effect of particle size on brain uranium distribution as a function of time.** Animals were exposed
 273 to UO_4 microparticles (white circles, blue dashed line) or to U metal nanoparticles (green squares, solid line) of
 274 uranium. Uranium concentrations were measured in olfactory bulbs (A), olfactory tubercles (B) and brain
 275 residue (C). Data are given as mean \pm SD of 8 animals. Significant difference from the respective timepoint
 276 $t=10$ min group is indicated as $^{\infty}p < 0.05$, $^{\infty\infty}p < 0.01$ and $^{\infty\infty\infty}p < 0.001$; significant difference from the respective
 277 timepoint $t=250$ min group is indicated as $^{\Delta}p < 0.05$; significant difference in between micro and nanoparticles
 278 group is indicated as $^*p < 0.05$ and $^{***}p < 0.001$ using two-way ANOVA (treatment x time) with the LSD
 279 *post hoc* test.

280

281 4. Discussion

282 Our study demonstrated that whatever the intrinsic characteristics of the U aerosol or its exposure, inhalation
 283 resulted in the presence of an important rostro-caudal gradient in the brain with the olfactory bulbs and the rest
 284 of the brain containing the highest and the lowest U concentration, respectively, confirming previous
 285 experiments (Houpert et al., 2007; Monleau et al., 2005; Tournier et al., 2009). However, the present
 286 investigation demonstrated that U distribution in the brain depends on several parameters: U aerosol
 287 concentration, U physico-chemical form such as its solubility, U particle size and the exposure number. Indeed,
 288 several factors affect the U concentrations as measured in tissues located in the frontal regions of the brain,
 289 closest to the nasal cavity on a neuroanatomical point of view (olfactory bulbs and tubercles). Data clearly
 290 demonstrated that the U concentration in the front of the brain is increased when animals are exposed to UO_2 , to
 291 a high concentration of UO_4 or to multiple exposures to UO_4 as compared to an acute UO_4 exposure. In addition,
 292 the kinetics of the U in the brain is modified by use of nanoparticles instead of microparticles. As a whole, our
 293 study shows that the ability of uranium to enter the brain depends on the conditions of inhalation in terms of
 294 aerosol concentration, the nature of the uranium and the frequency of exposure.

295 When U is inhaled, a fraction is found in the nasal cavity where a direct passage to the brain has been
 296 proposed, in addition to the transfer from the lungs via the bloodstream (Ibanez et al., 2014; Monleau et al.,
 297 2006; Tournier et al., 2009). The nasal cavity thus represents a potential route of entry of uranium to the brain.

298 We reported that only the High [UO₄] group shows an increase in the U concentration in the nasal turbinates
299 compared to the Low [UO₄] group, thus showing a dose effect of the aerosol concentration. Conversely, the
300 absence of a difference with the Low [UO₂] and Repeated low [UO₄] groups tends to show that the inhaled
301 quantity per exposure are comparable, which is in line with the concentrations measured in the generated
302 aerosols. It also demonstrates that there is no cumulative effect, from one day to the other, of the repeated
303 exposure at least in the nasal turbinates suggesting that nasal cavity probably flush away the aerosol within the
304 first 24 hours.

305

306 In the brain, we demonstrated that olfactory bulbs and tubercles are affected differently, unlike the rest of the
307 brain, probably because a lower U quantity reaching these more posterior brain regions (frontal cortex and brain
308 residue). These observations are in line with previous data (Ibanez et al., 2019; Monleau et al., 2005; Tournier et
309 al., 2009). In addition, the rostro-caudal gradient of the brain U distribution is modified by the repetition of
310 exposures. Indeed, in the Repeated low [UO₄] group, U levels were also found to be increased in the frontal
311 cortex but not in the rest of the brain. This observation is of particular interest since no cumulative effect was
312 observed in the nasal turbinates of the repeated group whereas U appears to cumulate in the olfactory bulbs and
313 even finally reach the frontal cortex which is not the case for an acute exposure. However, although group
314 differences are significant in brain areas, it is important to note that at the whole brain level, no group difference
315 appeared. These observations are also important in the sense that dose calculations to the brain in response to
316 exposure to a uranium aerosol do not consider the heterogeneity of the brain in terms of uranium accumulation.
317 Thus, even if the doses received globally by the brain are identical, some structures, located at the front of the
318 brain are more strongly exposed in case of inhalation. Therefore, brain toxicity calculations of U after inhalation
319 considering the brain as a homogeneous tissue may underestimate the real impact at more targeted brain areas.

320

321 The UO₂ (M/S) aerosol lead to a higher brain U accumulation in the olfactory bulbs and tubercles in
322 comparison with the UO₄ (F/M) aerosol, even if, at the whole brain level, no significant difference was observed.
323 These observations suggest that the olfactory pathway is taken by U particles, whether in soluble or insoluble
324 form. Physicochemical U forms in the tissue could differ from the original aerosol form once inhaled (Ibanez et
325 al., 2019). It is then possible that these chemical changes post-exposure could facilitate or prevent their
326 translocation to the brain. An impact of the solubility on the brain translocation was also reported for other
327 metals. As an example, solubility was shown to affect the manganese entry into the brain (Dorman et al., 2001;

328 Elder et al., 2006; Normandin et al., 2004). However, soluble forms of aluminium can better reach the brain than
329 insoluble forms (Chalansonnet et al., 2018). Thus, the solubility parameter of the aerosol alone may not be
330 sufficient to predict the ability of a particle to be transferred to the brain and that transfer assumptions should be
331 formulated carefully if risk assessments are to be carried out. Differences found in the literature could come from
332 a chemical property specific to each metal. In fact, several inhaled or instilled metals (eg aluminium, cadmium,
333 cobalt, thallium, manganese, zinc) can gain olfactory bulbs while others remain trapped in the nasal cavity (eg
334 iron and tungsten) (Henriksson et al., 1997; Kinoshita et al., 2008; Persson et al., 2003a; Persson et al., 2003b;
335 Radcliffe et al., 2009; Rao et al., 2003; Sunderman, 2001; Tjalve et al., 1996; Vitarella et al., 2000). And, once in
336 the brain some can migrate to more backward areas (Sunderman, 2001). Following a unilateral instillation the
337 difference between the ipsilateral and contralateral side is 395% for manganese but only 53% for aluminum
338 (Chalansonnet et al., 2018; Dorman et al., 2001).

339

340 Repeated exposure to uranium particles leads to a higher concentration in the brain, as a whole and in frontal
341 regions vs the brain residue. These data are consistent with the hypothesis that repeated exposure to uranium
342 leads to larger amounts in the frontal brain structures compared to acute exposure (olfactory bulbs and frontal
343 cortex) but also in cerebral structures spared by acute inhalation (olfactory tubercles). Our results show there
344 might be a cumulative effect of repeated exposures. Indeed, the Low group shows a concentration ratio between
345 OB and BRes of 1.44 on average vs 2.67 in the High group (see Supplemental Table 2). Thus, even if the
346 transfer from the lungs to the brain via the bloodstream contributes in the uranium concentrations within the
347 tissues, it is more likely that these gradients, and their amplitude, are due to the direct nose to brain passage.
348 Supporting this idea, we have previously shown that a peripheral injection of U does not give rise to a
349 preferential accumulation in any of the structures of the brain (Tournier et al., 2009).

350

351 As with microparticles, exposure with nanometric particles induced a higher U concentration at the front of
352 the brain. The data we observed agree with that obtained previously with the same exposure protocol (olfactory
353 brain: 1.65 ng/g in the previous study vs 1.44 ng/g in the present study) (Petitot et al., 2013). As for the
354 microparticles, metal-specific effects exist. For example in rodents, aluminum nanoparticles do not enter the
355 brain (Chalansonnet et al., 2018) while iron, manganese, zinc, among others, pass through the olfactory pathway
356 (Elder et al., 2006; Hopkins et al., 2018; Kao et al., 2012). Contradictory observations were also reported for

357 titanium dioxide nanoparticles capability to translocate to the brain after inhalation (Gate et al., 2017; Pujalte et
358 al., 2017).

359 For the reasons mentioned before, the microparticles- and nanoparticles-made aerosols differ widely and
360 cannot be directly compared. The data were therefore expressed in % of the measured concentration immediately
361 after the end of the inhalation period (t=10min). With this representation, we showed that the retention time in
362 the brain depends on the size of the particles: the nanoparticles are less easily cleared from the brain than the
363 microparticles in the three brain regions studied (OB, OT, BRes). In other words, the retention time and
364 therefore the duration of the contamination of U nanoparticles is longer than that of microparticles.

365 The kinetics of U microparticles in the brain appear to be closer to rubidium and thallium rather than that of
366 manganese, cadmium, cobalt, nickel and zinc. In fact, thallium has been shown to be rapidly transferred to the
367 OB, in less than 10 minutes (Kanayama et al., 2005). The kinetics of the rubidium concentration in OB was
368 evaluated at 3, 6, 12 and 24h in the brain after an intranasal administration and authors reported a gradually
369 decrease of the rubidium level throughout the 24h period (Kanayama et al., 2005). On the contrary, manganese,
370 cadmium and cobalt reach into the OB in around 24h (Brenneman et al., 2000; Persson et al., 2003b; Tjalve et
371 al., 1996). Regarding nickel or zinc, the metal peaks in OB were obtained only in 1 week after intranasal
372 administration (Henriksson et al., 1997; Persson et al., 2003a). Our observation of a longer retention time in the
373 case of nanoparticles is in line with previous observations. One study reported a greater retention of manganese
374 in the cortex and the same tendency in the olfactory bulb after inhalation of particles of 1 micron compared to 18
375 microns in mass median aerodynamic diameter (Fechter et al., 2002). A second study showed that inhaled
376 carbon nanoparticles remain present in the brain several days after the end of inhalation (Oberdorster et al.,
377 2004).

378

379 The concern of such direct translocation and retention of uranium particles into the brain is linked with its
380 dual chemical and radiotoxicity, as it is a transuranic element and an α emitter. In fact, cellular and cognitive
381 consequences may result from U exposure. In line with this idea, cognitive impairments were demonstrated in
382 rats following inhalation of aerosolized uranium (Monleau et al. 2005) and an inflammatory reaction was
383 observed in the spinal cord following chronic U ingestion (Saint-Marc et al., 2016). In addition, our data tend to
384 prove that physico-chemical changes of uranium particles (solubilized compounds, nanoparticles, ion forms) will
385 also need to be taken in account because they might influence subsequent neurotoxicity. Therefore, future
386 studies must be conducted to elucidate the physiological impact of inhaled U depending of its physico-chemical

387 form and particle size. In comparison, considering other metals, the association between particulate pollutants
388 inhalation and increased risk of deleterious effects on brain is a rising concern. Indeed, evidences that the brain
389 could be a direct target of inhalation exposures are piling up (Heusinkveld et al., 2016; Oberdorster et al., 2009),
390 and also concern human as Maher et al. observed magnetite particles of exogenous origin in the human brain
391 (Maher et al., 2016). More widely, deleterious effects of air pollution are thought to be mediated by the trigger of
392 neuroinflammation processes (Jayaraj et al., 2017) causing subsequent neurodegenerative disorders (Costa et al.,
393 2020).

394 Laboratory conditions with 56 mg/m³ of uranium in aerosol and 30 minutes continuous exposure represent
395 the “low” dose group compared to the other groups. This experimental dose was chosen according to the
396 technical constraints of the vaporization of the uranium powder and the stability of the aerosol formed and is,
397 therefore, not necessarily representative of the possible exposure values of populations with a risk of exposure.
398 However, it remains relatively low compared to previous experimental studies (between 190 and 412 mg/m³ and
399 between 30 and 120 min of exposition) (Monleau et al., 2006; Monleau et al., 2005; Tournier et al., 2009).

400

401 **5. Conclusions**

402 In conclusion, we have shown that the cerebral cartography of inhaled uranium has to be considered
403 according to a panel of parameters: its solubility, the frequency of the exposures, the concentration of the aerosol
404 and its granulometry. In all cases, a rostro-caudal gradient of uranium concentration from the olfactory bulbs to
405 the rest of the brain is observed. In each scenario of exposure, we showed that all these parameters modulate
406 either the concentrations, the brain regions involved or the retention time in the brain. These observations are of
407 importance as they demonstrate that brain dose calculations for uranium inhalation cannot be done in terms of
408 the whole brain effect but must consider the existence of a rostro-caudal gradient and the factors influencing it.
409 This study in rats supports the hypothesis in rodents of a direct transfer of inhaled U from the nasal cavity to the
410 brain, in addition to the supply through the bloodstream and bypassing the blood brain barrier. Further studies
411 will be necessary to demonstrate such a pathway in humans to determine whether the human dosimetry models
412 of ICRP for internal emitters (Leggett et al., 2018) should take this into account.

413

414 **Conflict of interest**

415 Authors have no conflict of interest to declare.

416

417 **Acknowledgement**

418 The authors wish to thank ORANO (AREVA NC) for partially supporting this work. They would also like to
419 thank Dr. François Gensdarmes for his advice for the generation of uranium nanoparticles.

420 **Supplemental data.**

421

	CTRL (Low)		CTRL (High)		CTRL (Ins.)		CTRL (Rep.)	
OB	1.06	±0.45	1.33	±0.33	1.56	±0.47	1.14	±1.28
OT	1.96	±0.36	2.78	±0.76	2.31	±0.51	2.21	±1.11
FCx	0.66	±0.38	0.85	±0.37	1.05	±0.42	0.65	±0.36
BRes	0.61	±0.05	0.69	±0.53	0.76	±0.69	0.71	±0.35

422

423 **Supplemental Table 1. Uranium concentrations in control groups.**

424 Quantification of uranium in the different control groups ([U] in ng/g of tissue). No difference was observed.

425 Data are indicated as mean ± SD (6-8 animals per group). *Abbreviations:* BRes, brain residue; FCx, frontal
426 cortex; OB, olfactory bulbs; OT, olfactory tubercles.

427

428

429

	CTRL		Low [UO₄]		High [UO₄]		Insoluble [UO₂]		Repeated low [UO₄]	
WB	0.75	±0.10**	2.46	±0.55	3.28	±0.36	3.00	±0.48	4.22	±0.51*
OB	1.31	±0.74*	2.61	±1.45	5.40	±1.06***	5.67	±2.68***	6.65	±2.97***
OT	2.34	±0.81	2.20	±1.30	4.52	±0.78***	5.60	±2.38*	5.46	±2.50**
FCx	0.81	±0.40*	2.15	±0.87	2.97	±1.82	2.65	±1.27	4.99	±1.91***
BRes	0.65	±0.48	1.81	±1.59	2.02	±1.01	2.00	±1.44	2.40	±1.09
NT	2.15	±5.00*	191	±186	1455	±648***	147	±49.7	362	±89.3
Kidneys	6.54	±3.43*	479	±246	10283	±1911***	69.6	±12.44	3730	±766***

430

431 **Supplemental Table 2. Uranium concentrations in the U microparticles treated rats.**

432 Quantification of uranium in the different groups at 24h after exposure to microparticles of uranium ([U] in ng/g
433 of tissue). Data are indicated as mean ± SD (8 animals per group). Difference from the Low [UO₄] group are
434 indicated at *p<0.05, **p<0.01, and ***p<0.001. *Abbreviations:* BRes, brain residue; FCx, frontal cortex; NT,
435 nasal turbinates; OB, olfactory bulbs; OT, olfactory tubercles; WB, whole brain.

436 **REFERENCES**

437

438 Ansoborlo, E., Prat, O., Moisy, P., Den Auwer, C., Guilbaud, P., Carriere, M., Gouget, B., Duffield, J., Doizi,
439 D., Vercouter, T., Moulin, C., Moulin, V., 2006. Actinide speciation in relation to biological processes.
440 *Biochimie* 88, 1605-1618.

441 Ballou, J.E., Gies, R.A., Case, A.C., Haggard, D.L., Buschbom, R.L., Ryan, J.L., 1986. Deposition and early
442 disposition of inhaled $^{233}\text{UO}_2(\text{NO}_3)_2$ and $^{232}\text{UO}_2(\text{NO}_3)_2$ in the rat. *Health Phys* 51, 755-771.

443 Barber, D.S., Ehrich, M.F., Jortner, B.S., 2005. The effect of stress on the temporal and regional distribution of
444 uranium in rat brain after acute uranyl acetate exposure. *J Toxicol Environ Health A* 68, 99-111.

445 Blanchin, N., Desloires, S., Grappin, L., Guillermin, A.M., Lafon, P., Miele, A., 2004. Protocoles de prise en
446 charge des incidents d'expositions internes au plutonium dans un service médical d'installation nucléaire de base
447 : élaboration - mise en place - évaluation - validation de 1996 à 2002. *Radioprotection* 39, 59-75.

448 Brenneman, K.A., Wong, B.A., Buccellato, M.A., Costa, E.R., Gross, E.A., Dorman, D.C., 2000. Direct
449 olfactory transport of inhaled manganese ($^{54}\text{MnCl}_2$) to the rat brain: toxicokinetic investigations in a
450 unilateral nasal occlusion model. *Toxicol Appl Pharmacol* 169, 238-248.

451 Chalansonnet, M., Carabin, N., Boucard, S., Merlen, L., Melczer, M., Antoine, G., Devoy, J., Remy, A.,
452 Gagnaire, F., 2018. Study of potential transfer of aluminum to the brain via the olfactory pathway. *Toxicol Lett*
453 283, 77-85.

454 Costa, L.G., Cole, T.B., Dao, K., Chang, Y.C., Coburn, J., Garrick, J.M., 2020. Effects of air pollution on the
455 nervous system and its possible role in neurodevelopmental and neurodegenerative disorders. *Pharmacol Ther*
456 210, 107523.

457 Craft, E., Abu-Qare, A., Flaherty, M., Garofolo, M., Rincavage, H., Abou-Donia, M., 2004. Depleted and natural
458 uranium: chemistry and toxicological effects. *J Toxicol Environ Health B Crit Rev* 7, 297-317.

459 Dewalle, P., Vendel, J., Weulersse, J.-M., Hervé, P., Decobert, G., 2010. Characterization of Aerosols Generated
460 by Nanosecond Laser Ablation of an Acrylic Paint. *Aerosol Science and Technology* 44, 902-915.

461 Diamond, G.L., Morrow, P.E., Panner, B.J., Gelein, R.M., Baggs, R.B., 1989. Reversible uranyl fluoride
462 nephrotoxicity in the Long Evans rat. *Fundam Appl Toxicol* 13, 65-78.

463 Dinocourt, C., Legrand, M., Dublineau, I., Lestaevel, P., 2015. The neurotoxicology of uranium. *Toxicology*
464 337, 58-71.

465 Dorman, D.C., Struve, M.F., James, R.A., Marshall, M.W., Parkinson, C.U., Wong, B.A., 2001. Influence of
466 particle solubility on the delivery of inhaled manganese to the rat brain: manganese sulfate and manganese
467 tetroxide pharmacokinetics following repeated (14-day) exposure. *Toxicol Appl Pharmacol* 170, 79-87.

468 Durakovic, A., Horan, P., Dietz, L.A., Zimmerman, I., 2003. Estimate of the time zero lung burden of depleted
469 uranium in Persian Gulf War veterans by the 24-hour urinary excretion and exponential decay analysis. *Mil Med*
470 168, 600-605.

471 Elder, A., Gelein, R., Silva, V., Feikert, T., Opanashuk, L., Carter, J., Potter, R., Maynard, A., Ito, Y.,
472 Finkelstein, J., Oberdorster, G., 2006. Translocation of inhaled ultrafine manganese oxide particles to the central
473 nervous system. *Environ Health Perspect* 114, 1172-1178.

474 Fechter, L.D., Johnson, D.L., Lynch, R.A., 2002. The relationship of particle size to olfactory nerve uptake of a
475 non-soluble form of manganese into brain. *Neurotoxicology* 23, 177-183.

476 Fulco, C.E., Liverman, C.T., Sox, H.C., 2000. Depleted uranium, Pyridostigmine bromide, Sarin and Vaccines.
477 In: Depleted Uranium. . Gulf War and Health National Academies press, Washington 1, 89-168.

478 Gate, L., Disdier, C., Cosnier, F., Gagnaire, F., Devoy, J., Saba, W., Brun, E., Chalansonnet, M., Mabondzo, A.,
479 2017. Biopersistence and translocation to extrapulmonary organs of titanium dioxide nanoparticles after
480 subacute inhalation exposure to aerosol in adult and elderly rats. *Toxicol Lett* 265, 61-69.

481 Henriksson, J., Talkvist, J., Tjalve, H., 1997. Uptake of nickel into the brain via olfactory neurons in rats.
482 *Toxicol Lett* 91, 153-162.

483 Heusinkveld, H.J., Wahle, T., Campbell, A., Westerink, R.H.S., Tran, L., Johnston, H., Stone, V., Cassee, F.R.,
484 Schins, R.P.F., 2016. Neurodegenerative and neurological disorders by small inhaled particles. *Neurotoxicology*
485 56, 94-106.

486 Hopkins, L.E., Laing, E.A., Peake, J.L., Uyeminami, D., Mack, S.M., Li, X., Smiley-Jewell, S., Pinkerton, K.E.,
487 2018. Repeated Iron-Soot Exposure and Nose-to-brain Transport of Inhaled Ultrafine Particles. *Toxicol Pathol*
488 46, 75-84.

489 Houpert, P., Frelon, S., Monleau, M., Bussy, C., Chazel, V., Paquet, F., 2007. Heterogeneous Accumulation Of
490 Uranium In The Brain Of Rats. *Radiat Prot Dosimetry*.

491 Houpert, P., Lestaevel, P., Bussy, C., Paquet, F., Gourmelon, P., 2005. Enriched but not depleted uranium affects
492 central nervous system in long-term exposed rat. *Neurotoxicology* 26, 1015-1020.

493 Ibanez, C., Suhard, D., Elie, C., Ebrahimian, T., Lestaevel, P., Roynette, A., Dhieux-Lestaevel, B., Gensdarmes,
494 F., Tack, K., Tessier, C., 2019. Evaluation of the Nose-to-Brain Transport of Different Physicochemical Forms
495 of Uranium after Exposure via Inhalation of a UO₄ Aerosol in the Rat. *Environ Health Perspect* 127, 97010.

496 Ibanez, C., Suhard, D., Tessier, C., Delissen, O., Lestaevel, P., Dublineau, I., Gourmelon, P., 2014. Intranasal
497 exposure to uranium results in direct transfer to the brain along olfactory nerve bundles. *Neuropathol Appl*
498 *Neurobiol* 40, 477-488.

499 ICRP, 1994. Human Respiratory Tract Model for Radiological Protection. ICRP Publication 66. *Ann ICRP* 24
500 (1-3).

501 ICRP, 2017. Occupational intakes of radionuclides: Part 3. ICRP Publication 137. *Ann ICRP* 46(3/4).

502 Jayaraj, R.L., Rodriguez, E.A., Wang, Y., Block, M.L., 2017. Outdoor Ambient Air Pollution and
503 Neurodegenerative Diseases: the Neuroinflammation Hypothesis. *Curr Environ Health Rep* 4, 166-179.

504 Kanayama, Y., Enomoto, S., Irie, T., Amano, R., 2005. Axonal transport of rubidium and thallium in the
505 olfactory nerve of mice. *Nucl Med Biol* 32, 505-512.

506 Kao, Y.Y., Cheng, T.J., Yang, D.M., Wang, C.T., Chiung, Y.M., Liu, P.S., 2012. Demonstration of an olfactory
507 bulb-brain translocation pathway for ZnO nanoparticles in rodent cells in vitro and in vivo. *J Mol Neurosci* 48,
508 464-471.

509 Kinoshita, Y., Shiga, H., Washiyama, K., Ogawa, D., Amano, R., Ito, M., Tsukatani, T., Furukawa, M., Miwa,
510 T., 2008. Thallium transport and the evaluation of olfactory nerve connectivity between the nasal cavity and
511 olfactory bulb. *Chem Senses* 33, 73-78.

512 La Touche, Y.D., Willis, D.L., Dawydiak, O.I., 1987. Absorption and biokinetics of U in rats following an oral
513 administration of uranyl nitrate solution. *Health Phys* 53, 147-162.

514 Leggett, R.W., Eckerman, K.F., Bellamy, M., 2018. MPS dose reconstruction for internal emitters: some site-
515 specific issues and approaches. *Int J Radiat Biol*, 1-13.

516 Lemercier, V., Millot, X., Ansoborlo, E., Menetrier, F., Flury-Herard, A., Rousselle, C., Scherrmann, J.M., 2003.
517 Study of uranium transfer across the blood-brain barrier. *Radiat Prot Dosimetry* 105, 243-245.

518 Maher, B.A., Ahmed, I.A., Karloukovski, V., MacLaren, D.A., Foulds, P.G., Allsop, D., Mann, D.M., Torres-
519 Jardon, R., Calderon-Garciduenas, L., 2016. Magnetite pollution nanoparticles in the human brain. *Proc Natl*
520 *Acad Sci U S A* 113, 10797-10801.

521 Monleau, M., Blanchardon, E., Claraz, M., Paquet, F., Chazel, V., 2006. The effect of repeated inhalation on the
522 distribution of uranium in rats. *J Toxicol Environ Health A* 69, 1629-1649.

523 Monleau, M., Bussy, C., Lestaevel, P., Houpert, P., Paquet, F., Chazel, V., 2005. Bioaccumulation and
524 behavioural effects of depleted uranium in rats exposed to repeated inhalations. *Neurosci Lett* 390, 31-36.

525 Normandin, L., Ann Beaupre, L., Salehi, F., St -Pierre, A., Kennedy, G., Mergler, D., Butterworth, R.F.,
526 Philippe, S., Zayed, J., 2004. Manganese distribution in the brain and neurobehavioral changes following
527 inhalation exposure of rats to three chemical forms of manganese. *Neurotoxicology* 25, 433-441.

528 Oberdorster, G., Elder, A., Rinderknecht, A., 2009. Nanoparticles and the brain: cause for concern? *J Nanosci*
529 *Nanotechnol* 9, 4996-5007.

530 Oberdorster, G., Sharp, Z., Atudorei, V., Elder, A., Gelein, R., Kreyling, W., Cox, C., 2004. Translocation of
531 inhaled ultrafine particles to the brain. *Inhal Toxicol* 16, 437-445.

532 Onodera, J., Yabuta, H., Nishizoro, T., Nakamura, C., Ikezawa, Y., 1991. Characterization of aerosols from
533 dismantling work of experimental nuclear power reactor decommissioning. *Journal of Aerosol Science* 22, S747-
534 S750.

535 Paquet, F., Houpert, P., Blanchardon, E., Delissen, O., Maubert, C., Dhieux, B., Moreels, A.M., Frelon, S.,
536 Gourmelon, P., 2006. Accumulation and distribution of uranium in rats after chronic exposure by ingestion.
537 *Health Phys* 90, 139-147.

538 Persson, E., Henriksson, J., Tallkvist, J., Rouleau, C., Tjalve, H., 2003a. Transport and subcellular distribution of
539 intranasally administered zinc in the olfactory system of rats and pikes. *Toxicology* 191, 97-108.

540 Persson, E., Henriksson, J., Tjalve, H., 2003b. Uptake of cobalt from the nasal mucosa into the brain via
541 olfactory pathways in rats. *Toxicol Lett* 145, 19-27.

542 Petitot, F., Lestaevel, P., Tourlonias, E., Mazzucco, C., Jacquinet, S., Dhieux, B., Delissen, O., Tournier, B.B.,
543 Gensdarmes, F., Beaunier, P., Dublineau, I., 2013. Inhalation of uranium nanoparticles: respiratory tract
544 deposition and translocation to secondary target organs in rats. *Toxicol Lett* 217, 217-225.

545 Pujalte, I., Dieme, D., Haddad, S., Serventi, A.M., Bouchard, M., 2017. Toxicokinetics of titanium dioxide
546 (TiO₂) nanoparticles after inhalation in rats. *Toxicol Lett* 265, 77-85.

547 Radcliffe, P.M., Olabisi, A.O., Wagner, D.J., Leavens, T., Wong, B.A., Struve, M.F., Chapman, G.D., Wilfong,
548 E.R., Dorman, D.C., 2009. Acute sodium tungstate inhalation is associated with minimal olfactory transport of
549 tungsten (188W) to the rat brain. *Neurotoxicology* 30, 445-450.

550 Rao, D.B., Wong, B.A., McManus, B.E., McElveen, A.M., James, A.R., Dorman, D.C., 2003. Inhaled iron,
551 unlike manganese, is not transported to the rat brain via the olfactory pathway. *Toxicol Appl Pharmacol* 193,
552 116-126.

553 Saint-Marc, B., Elie, C., Manens, L., Tack, K., Benderitter, M., Gueguen, Y., Ibanez, C., 2016. Chronic uranium
554 contamination alters spinal motor neuron integrity via modulation of SMN1 expression and microglia
555 recruitment. *Toxicol Lett* 254, 37-44.

556 Salbu, B., Janssens, K., Lind, O.C., Proost, K., Gijssels, L., Danesi, P.R., 2005. Oxidation states of uranium in
557 depleted uranium particles from Kuwait. *J Environ Radioact* 78, 125-135.

558 Sunderman, F.W., Jr., 2001. Nasal toxicity, carcinogenicity, and olfactory uptake of metals. *Ann Clin Lab Sci*
559 31, 3-24.

560 Tjalve, H., Henriksson, J., Tallkvist, J., Larsson, B.S., Lindquist, N.G., 1996. Uptake of manganese and
561 cadmium from the nasal mucosa into the central nervous system via olfactory pathways in rats. *Pharmacol*
562 *Toxicol* 79, 347-356.

563 Tournier, B.B., Frelon, S., Tournalias, E., Agez, L., Delissen, O., Dublineau, I., Paquet, F., Petitot, F., 2009.
564 Role of the olfactory receptor neurons in the direct transport of inhaled uranium to the rat brain. *Toxicol Lett*
565 190, 66-73.

566 Trelenberg, T.W., Glade, S.C., Tobin, J.G., Hamza, A.V., 2006. The production and oxidation of uranium
567 nanoparticles produced via pulsed laser ablation. *Surface Science* 600, 2338-2348.

568 UNSCEAR, A.D., 2016. Biological effects of selected internal emitters-uranium.

569 Vitarella, D., Wong, B.A., Moss, O.R., Dorman, D.C., 2000. Pharmacokinetics of inhaled manganese phosphate
570 in male Sprague-Dawley rats following subacute (14-day) exposure. *Toxicol Appl Pharmacol* 163, 279-285.

571